Detection of the Short-Circuit Faults in the Stator Winding of Induction Motors based on Harmonics of the Neighboring Magnetic Field

V. Fireteanu[1]
[1]EPM_NM Laboratory, POLITEHNICA University of Bucharest,
313 Splaiul Independentei, 060042, Bucharest, Romania

E-mail: virgiliu.fireteanu@upb.ro

Abstract. Based on the time domain finite element analysis of the electromagnetic field, this paper studies the signature of the short-circuit faults inside the stator winding in the magnetic field outside induction motors. The detection of the such a fault is based on the evaluation of the output voltage of coil sensors placed in the motors neighbouring and the comparison of amplitudes of harmonics of this voltage for the healthy and faulty operation states.

1. Introduction

The study based on finite element models offers much more information on the phenomena characterizing the operation of electrical machines than the classical analytical models. This explains the increase of the interest for the finite element investigations in electrical machines [1-10].
Based on finite element models [5], this paper studies the influence on the magnetic field outside induction motors of a short-circuit fault in the stator winding. The neighbouring magnetic field is investigated through the harmonics in the time variation of the output voltage of coil sensors in case of healthy and faulty motor states, for no-load and for loaded motor operation.

2. Dedicated time domain finite element field-circuit model of induction motors

The geometry and mesh of the electromagnetic field 2D computation domain, Fig. 1(a), (b) and the circuit model, Fig. 1 (c), belong to a four poles squirrel cage induction motor of 11 kW, 3 x 380 V, f_n = 50 Hz supplied. This domain contains the stator and the rotor cores, which are magnetic and nonconductive regions, the 48 stator slots - nonconductive, nonmagnetic and source regions, the 32 bars of the rotor squirrel cage aluminum made, the nonmagnetic motor frame of 8 mm thickness and the motor shaft, which are regions of solid conductor type, the motor airgap and an infinitely extended air region outside the motor. In order to investigate the neighboring magnetic field, the computation domain includes two coil sensors with a common magnetic core, the radial sensor *SensorOx*, blue colored, and the azimuth sensor *SensorOy*, in red, Fig. 1 (b).
The Phase B and the Phase C of the stator winding are represented in the circuit model, Fig. 1 (c), by four coil components, which reflects the four groups representing each the four go- and the four return

sides of the elementary coils, Fig. 1 (a). Each elementary coil occupies two stator slots and four elementary coils series connected represent one pole of the stator winding.
It is the Phase A, Fig. 1 (c), of the stator winding where the short-circuit fault is considered. The section of this winding representing one stator pole, which regroups four elementary coils in red in Fig. 1 (a), is represented in the circuit model, Fig. 1 (c), through eight coil components. These are the go-sides and the return sides of four elementary coils. The resistor R in the circuit model, Fig. 1 (c), is used to simulate the short-circuit of the one of the elementary coils of the Phase A. The go-side of the elementary coil in short-circuit is placed around the Ox axis, Fig. 1 (b), (a).

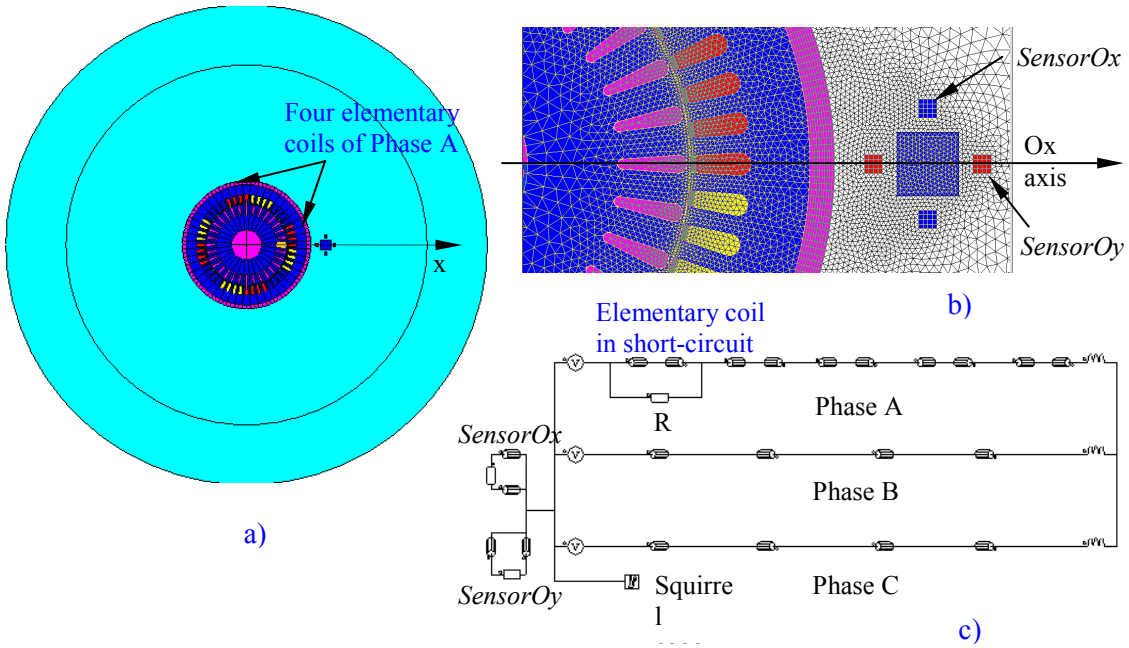

Figure 1. Geometry (a) and mesh (b) of the computation domain and the circuit model (c)

The circuit model includes for each of the two coil sensors, *SensorOx* and *SensorOy*, Fig. 1 (c), two coil components and a resistor of high resistance for the evaluation of sensors output voltage.
The magnetic vector potential $\boldsymbol{A}(x,y,z,t)$, which is the state variable of the electromagnetic field, satisfies the differential equations:

$$\operatorname{curl}\left[1/\mu \cdot \operatorname{curl} \boldsymbol{A}\right] + \left(\partial \boldsymbol{A}/\partial t\right)/\rho = \boldsymbol{J}_s\left(x,y,z,t\right);\ \operatorname{div} \boldsymbol{A} = 0 \qquad (1)$$

where μ is the magnetic permeability, ρ is the resistivity and $\boldsymbol{J}_s$ is the current density in the stator slots. The term $(\partial \boldsymbol{A}/\partial t)/\rho$ reflects the density of the induced current in the regions of solid conductor type.
In the 2D field model considered in this paper the source current density has the structure $\boldsymbol{J}_s[0,\ 0,\ J_s(x,y,t)]$. As consequence, the vector potential $\boldsymbol{A}[0,\ 0,\ A_s(x,y,t)]$ is oriented normal on the xOy plane and does not depends on the third coordinate of the Cartesian coordinate system (x, y, z).
The investigation of the electromagnetic field inside and outside the motor uses a transient magnetic model of induction motors [10, 11]. This time domain analysis of the electromagnetic field considers the imposed constant rotor speed, 1450 rpm for the rated load motor operation, and the synchronous speed 1500 rpm for the ideal no-load motor operation.

3. Signature of the short-circuit fault in the magnetic field outside the motors

This section analyses results related the time variation of the output voltage of *SensorOx* and *SensorOy* coil sensors when pass from the healthy state (HE) to the short-circuit faulty state (FA) of

motor operation. The changes in amplitude of harmonics of this voltage in the range [500 … 1000] Hz are evaluated.

No-load motor operation. The amplitude of the main harmonics of the *SensorOx* voltage in the range [500 ... 1000] Hz, Fig. 2, have an important increase when pass from the healthy state (HE0) to the faulty state (FA0). The ratio FA0/HE0 of the amplitudes, Table 1, shows that the most important increase is reflected by the 650 Hz harmonic, followed by the harmonic with the frequency 850 Hz.

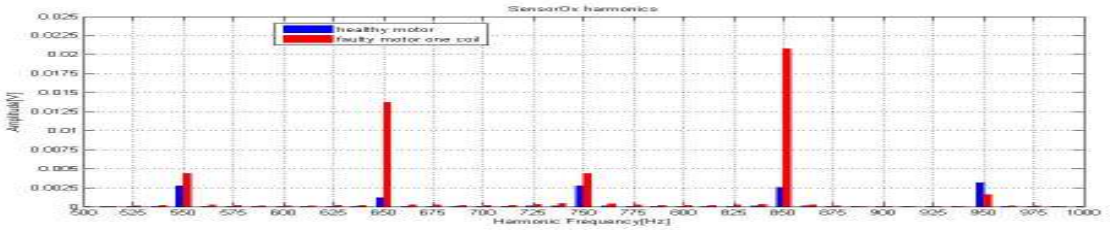

Figure 2. Amplitude of harmonics of *SensorOx* voltage.

Table 1. Amplitude of harmonics of *SensorOx* voltage, no-load operation (1500 rpm)

f [Hz]	550	650	750	850	950
HE0 [mV]	2.729	1.163	2.726	2.52	3.146
FA0 [mV]	4.382	13.72	4.355	20.75	1.625
FA0/HE0	1.61	11.8	1.60	8.23	0.516

In case of the *SensorOy* voltage, Fig. 3, the most important increase, 9.37 times, characterizes the amplitude of the same 650 Hz harmonic. Consequently, *SensorOx* and *SensorOy* offer similar efficiency of fault detection based on the criterion FA0/HE0. For the most important harmonics this ratio increases around 10 times.

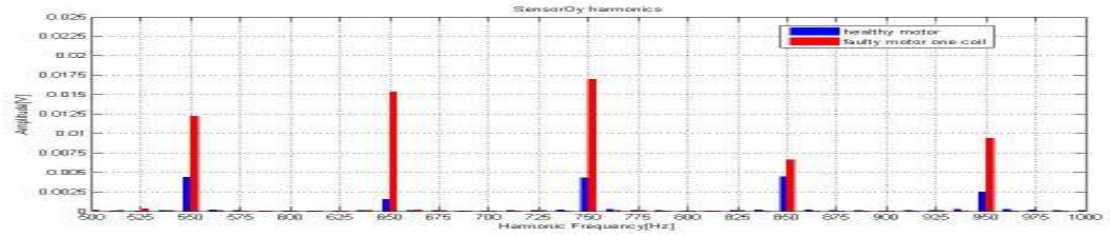

Figure 3. Amplitude of harmonics of *SensorOy* voltage.

Loaded motor operation. The amplitude of the main harmonics of the *SensorOx* voltage generally decreases. It is the case of the 625 Hz harmonic, with the value 0.79 of the ratio FA1/HE1, Table 2. In case of the *SensorOy* voltage the decrease of the amplitude of the 925 Hz harmonic is much more important, around 8 times from the healthy state to the faulty state of the motor, Table 2.

Table 2. Ratio FA1/HE1 of amplitude decrease, loaded motor operation (1450 rpm)

f [Hz]	525	625	725	825	925
SensorOx	0.84	0.79	0.99	1.05	0.92
SensorOy	0.47	0.734	0.36	0.134	0.130

4. Detection of the short-circuit fault with increased efficiency

In accordance with the results in the section 3, the on-line detection of the short-circuit fault in the stator winding consists in the survey of the amplitude of a particular harmonic of the output voltage of *SensorOx* or of *SensorOy* coil sensors. For the no-load motor operation the appropriate harmonic has the frequency 650 Hz. In case of loaded motor operation, the harmonic of 925 Hz of the *SensorOy* voltage can be used.

A much more efficient solution for short-circuit fault detection uses two groups of two coils placed at the same distance from the motor axis. The first group consists in the coils *SensorOx*, *SensorOy*, and the second group in the coils *Sensor2Ox*, *Sensor2Oy*, Fig. 4 (a). The second group of two coils is shifted 90 degrees around the motor axis with respect the first group. The two coils *SensorOx*, *Sensor2Ox* and the two coils *SensorOy*, *Sensor2Oy* are series connected. The new output voltages, denominated *SensorsOx+2Ox* and *SensorsOy+2Oy*, Fig. 4 (b), will be further evaluated.
The azymuth position of the four coils system with respect the motor is defined by the angle Alpha, Fig. 4 (a), between the horizonthal Ox axys and the radial line that connect the center of the *SensorOx, SensorOy* assembly and the center O of the motor.

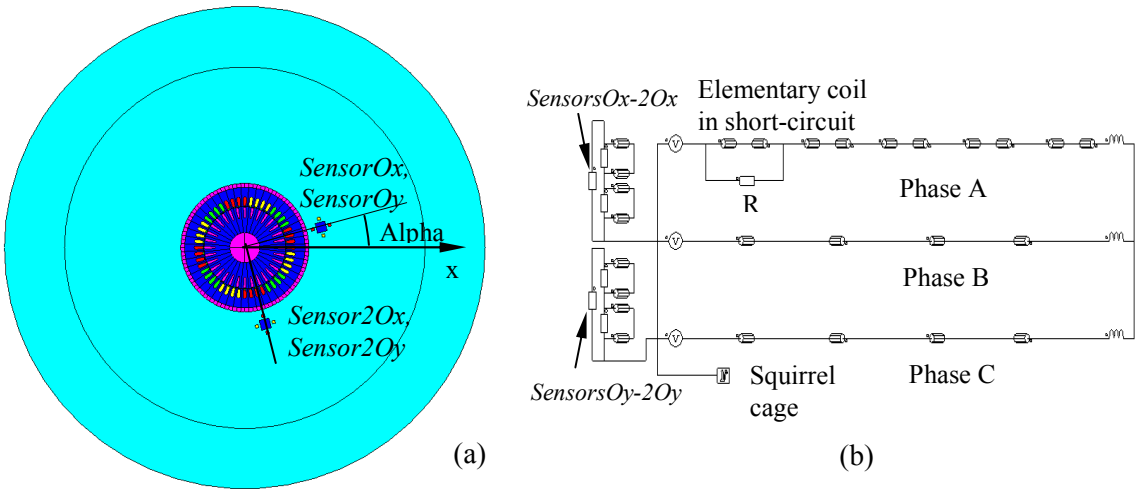

Figure 4. Computation domain geometry (a) for Alpha = 15 degrees and the new circuit model (b)

The numerical results in Tables 3, 4 for Alpha = 15 degrees related the ratio between the amplitude of the main harmonics of *SensorsOx+2Ox* and *SensorsOy+2Oy* voltages, FE0/HA0 for no-load motor operation and FE1/HA1 for loaded motor operation, offers the following findings:

- the efficiency of fault detection through the *SensorsOx+2Ox* and *SensorsOy+2Oy* voltages is much more higher than through the *SensorOx* and *SensorOy* voltages;
- for the no-load motor operation, the efficiency of fault detection through the *SensorsOy+2Oy* voltage is higher than through the *SensorsOx+2Ox* voltage. The maximum of this efficiency, FE0/HA0 = 5115 corresponds to the harmonics of 650 Hz;
- for loaded motor operation, the efficiency of fault detection is lower. The *SensorsOx+2Ox* is the best solution and the maximum efficiency, FE1/HA1 = 730.7 it is obtained with the 625 Hz harmonic.

Table 3. Ratio FA0/HE0 of amplitudes, no-load motor operation (1500 rpm)

f [Hz]	550	650	750	850	950
SensorsOx+2Ox	310.9	522.8	757.0	1155.2	818.5
SensorsOy+2Oy	2935	5115	2668	3249	2043

Table 4. Ratio FA1/HE1 of amplitudes, loaded motor operation (1450 rpm)

f [Hz]	525	625	725	825	925
SensorsOx+2Ox	574.4	730.7	396.4	476.6	367.4
SensorsOy+2Oy	45.31	187.0	110.1	123.2	91.99

5. Identification of the short-circuit position and maximum of the fault detection efficiency

The next tables contain results related the value of the amplitude of the 650 Hz, 750 Hz and 850 Hz harmonics of *SensorsOx+2Ox* and *SensorsOy+2Oy* voltages, which are the main harmonics in case of

no-load motor operation and of the 625 Hz, 725 Hz and 825 Hz harmonics, which are the main harmonics in case of loaded motor operation. The maximum in the dependence of the harmonics amplitude on the azimuth position of coil sensors corresponds to Alpha = 0 degrees, if the *SensorOx+2Ox* voltage is used for the no-load motor operation, Table 5, and if the *SensorOy+2Oy* voltage is used for the loaded motor operation, Table 8.
The minimum in the dependence of the amplitude of the main harmonics with respect the azimuth position of the coil sensors corresponds to the value Alpha = 90 degrees, Tables 7, 8, for the loaded motor operation in both cases, *SensorOx+2Ox* and *SensorOy+2Oy*.
For the detection of the position of the elementary coil in short-circuit remember that the go-side position of this coil corresponds to Alpha = 0, Fig. 4 (a). In this context, the maximum of the amplitude of the 750 Hz harmonic of *SensorOx+2Ox* for no-load motor operation, Table 5, and of the 725 Hz harmonic of *SensorOy+2Oy* for loaded motor operation, Table 8, corresponds also to Alpha = 0 degrees. The minimum of the amplitude of these harmonics corresponds to Alpha = 90 degrees.

Table 5. Amplitude of *SensorOx+2Ox* harmonics, no-load motor operation (1500 rpm)

Alpha[degrees]	-15	0	15	30	45	60	75	90	105
Harm_650 Hz ampli mV]	16.5	19.9	8.78	4.73	5.03	2.73	1.07	0.59	0.56
Harm_750 Hz ampli [mV]	7.85	23.7	16.2	6.23	3.69	2.71	1.14	0.54	2.62
Harm_850 Hz ampli [mV]	6.51	29.9	14.4	4.05	4.25	3.51	1.74	1.99	3.68

Table 6. Amplitude of *SensorOy+2Oy* harmonics, no-load motor operation (1500 rpm)

Alpha[degrees]	-15	0	15	30	45	60	75	90	105
Harm_650 Hz ampli [mV]	33.7	18.7	11.9	2.66	3.54	2.45	0.78	0.89	1.12
Harm_750 Hz ampli [mV]	40.0	12.8	9.56	11.7	6.50	2.19	1.48	2.47	3.62
Harm_850 Hz ampli [mV]	40.5	6.78	12.0	10.0	5.03	1.36	1.48	2.10	3.65

Table 7. Amplitude of *SensorOx+2Ox* harmonics, loaded motor operation (1450 rpm)

Alpha[degrees]	-15	0	15	30	45	60	75	90	105
Harm_625 Hz ampli [mV]	27.5	5.97	25.9	7.49	3.30	1.89	1.08	0.61	1.81
Harm_725 Hz ampli [mV]	33.8	3.48	35.4	8.25	2.32	1.69	1.14	0.30	1.05
Harm_825 Hz ampli [mV]	41.3	1.79	41.2	13.8	4.97	2.38	0.84	0.72	2.01

Table 8. Amplitude of *SensorOy+2Oy* harmonics, loaded motor operation (1450 rpm)

Alpha[degrees]	-15	0	15	30	45	60	75	90	105
Harm_625 Hz ampli [mV]	2.81	64.3	7.46	6.27	3.77	1.86	1.52	1.04	1.04
Harm_725 Hz ampli [mV]	0.53	81.0	8.39	10.0	4.10	1.20	1.64	0.82	1.55
Harm_825 Hz ampli [mV]	2.29	95.9	5.38	9.04	5.88	4.18	0.97	0.42	2.49

In the context of on-line survey of the healthy state of the elementary coil considered for the short-circuit fault investigation, the results in Tables 9 and 10 show that the maximum efficiency of the faulty state detection based on the amplitude of the 750 Hz harmonic of the *SensorOx+2Ox* voltage for no-load motor operation, Table 9, and of the 725 Hz harmonic of the *SensorOy+2Oy* voltage for loaded motor operation, Table 10, corresponds to Alpha = 0 degrees.

Table 9. Efficiency of fault detection through the 750 Hz harmonic of *SensorOx+2Ox* voltage, no-load motor operation (1500 rpm)

Alpha[degrees]	-15	0	15	30	45	60	75	90	105
FA0/HE0	351.8	1296.2	757.0	311.6	182.5	165.3	51.3	30.0	117.1

Table 10. Efficiency of fault detection through the 725 Hz harmonic of *SensorOy+2Oy* voltage, loaded motor operation (1450 rpm)

Alpha[degrees]	-15	0	15	30	45	60	75	90	105
FA0/HE0	6.94	1169.0	110.1	137.3	55.5	16.6	21.5	11.7	20.6

6. Conclusions

The detection of the short-circuit in the stator winding of induction motors can be the result of the comparison of the amplitudes for healthy and faulty motor operation states of harmonics of the output voltage of a neighbouring coil sensor, radial or azimuthally orientated with respect the motor.
An increased efficiency of the fault detection and the possibility to detect the azimuth position of the short-circuit fault inside the stator are offered by a system of two coil sensors series connected, one pole shifted around the motor.

7. References

[1] J. Penman, H.G. Sedding and W.T. Fink, “Detection and location of inter-turn short circuits in the stator windings of operating motors,” *IEEE Trans. Energy Conversion.*, vol. 9, No. 4, pp. 652-658, Dec. 1994.
[2] H. Henao, C. Demian, and G.A. Capolino, “A frequency-domain detection of stator winding faults in induction machines using an external flux sensor”, *IEEE Trans. Ind. Appl.*, vol. 39, pp. 1272–1279, Sept/Oct. 2003.
[3] T. Assaf, H. Henao, G.A. Capolino, “Simplified axial flux spectrum method to detect incipient stator inter-turn short-circuits in induction machine”, in *Proc. IEEE ISIE. 2004*, Ajaccio, France, pp. 815–819, vol. 2, 2004.
[4] M. D. Negrea, “Electromagnetic Flux Monitoring for Detecting Faults in Electrical Machines”, doctoral disertation at Helsinki University of Technology, Laboratory of Electromechanics, November, 2006.
[5] V. Fireteanu, P. Taras, “Teaching induction machine through finite element models”, *Proc. of XVIII ICEM Conf.*, Sept. 6-9, 2008, Vilamoura, Portugual.
[6] B. Vaseghi, N. Takorabet, and F. Meibody-Tabar, "Transient finite element analysis of induction machines with stator winding turn fault," *Progress In Electromagnetics Research (PIER) Journals,* vol. 95, pp. 1-18, 2009.
[7] A. Ceban, “Methode globale de diagnostique des machines electriques” , PhD Thesis, LSEE Lab., Université d’Artois, France 2012.
[8] L. Frosini, A. Borin, L. Girometta, G. Venchi, “A novel approach to detect short circuits in low voltage induction motor by stray flux measurement”, *Proc. of ICEM Conf.,* September 2-5, 2012, Marseille, France.
[9] R. Pusca, R. Romary, A. Ceban, “Detection of inter-turn short circuits in induction machines without knowledge of the healthy state”, *Proc. of ICEM Conf.,* September 2-5, 2012, Marseille, France.
[10] A-I. Constantin, V. Fireteanu, V. Leconte, “Effects of the short-circuit faults in the stator winding of induction motors and fault detection through the magnetic field harmonics, *Proc. of ATEE Conf.,* May 23-25, 2013, Bucharest, Romania.
[11] V. Fireteanu, A-I. Constantin, R. Romary, R. Pusca, S. Ait-Amar, “Finite element investigation of the short-circuit fault in the stator winding of induction motors and harmonics of the neighboring magnetic field”, *Proc. of SDEMPED Symp.,* August 27-30, 2013, Valencia, Spain.